The Astrophysical Journal Letters, 746:L5 (7pp), 2012 February 10 doi:10.1088/2041-8205/746/1/L5

OBSERVATIONS OF A TWO-STAGE SOLAR ERUPTIVE EVENT (SEE): EVIDENCE FOR SECONDARY HEATING

Yang Su[1,2,3], Brian R. Dennis[1], Gordon D. Holman[1], Tongjiang Wang[1,2], Phillip C. Chamberlin[1], Sabrina Savage[1], and Astrid Veronig[3]
[1] Solar Physics Laboratory (Code 671), Heliophysics Science Division, NASA Goddard Space Flight Center, Greenbelt, MD 20771, USA; yang.su@uni-graz.at
[2] Department of Physics, The Catholic University of America, Washington, DC 20064, USA
[3] Institute of Physics, University of Graz, Universitaetsplatz 5, Graz 8010, Austria
Received 2011 August 30; accepted 2012 January 5; published 2012 January 19

ABSTRACT

We present *RHESSI*, *SDO*/AIA, *SOHO*/LASCO, *STEREO*, and *GOES* observations of a partially occulted solar eruptive event that occurred at the southwest limb on 2011 March 8. The *GOES* X-ray light curve shows two peaks separated by almost 2 hr that we interpret as two stages of a single event associated with the delayed eruption of a coronal mass ejection (CME). A hot flux rope formed during the first stage and continued expanding and rising throughout the event. The speed of the flux rope decreased from ∼120 to 14 km s^{-1} during the decay phase of the first stage and increased again during the second stage to become the CME with a speed of ∼516 km s^{-1}. *RHESSI* and *GOES* data analyses show that the plasma temperature reached over 20 MK in the first stage, then decreased to ∼10 MK and increased to 15 MK in the second stage. This event provides clear evidence for a secondary heating phase. The enhanced EUV and X-ray emission came from the high corona (∼60 arcsec above the limb) in the second stage, ∼40 arcsec higher than the site of the initial flare emission. *STEREO-A* on-disk observations indicate that the post-flare loops during this stage were of larger scale sizes and spatially distinct from those in the first stage.

Key words: Sun: coronal mass ejections (CMEs) – Sun: flares – Sun: UV radiation – Sun: X-rays, gamma rays

Online-only material: animations, color figures

1. INTRODUCTION

In the standard model of an impulsive solar flare (see, for example, Shibata et al. 1995; Shibata 1998; Tsuneta 1997), energy is released from the coronal magnetic field by a reconnection process. As a result, plasma is heated to $\gtrsim$10 MK and particles—electrons and ions—are accelerated to relativistic energies. When the flare is accompanied by an eruption, i.e., a jet or a coronal mass ejection (CME), the event is known as a solar eruptive event (SEE). These are the most geoeffective events, since they can subsequently affect Earth's space environment.

Based on observations from the full-Sun EUV Variability Experiment (EVE; Woods et al. 2010) on the *Solar Dynamics Observatory* (*SDO*), Woods et al. (2011) have shown the existence of large secondary peaks in the EUV light curves of some flares that can occur many minutes to hours after the initial impulsive energy release that, in other respects, appear to be consistent with the standard flare model. They have argued that, in some cases, these secondary peaks represent additional episodes of energy release in the corona that heat plasma to temperatures of a few MK. Not only are the secondary peaks delayed in time from the impulsive emission, but they have larger scale sizes (based on *SDO*/Atmospheric Imaging Assembly (AIA) images in the EUV), indicating a significantly higher altitude than the site of the earlier, more impulsive emission. However, since these reported secondary events are significantly cooler than the initially heated plasma and are not detected in *GOES* soft X-ray light curves, there is always the possibility that they merely reflect the cooling of the previously heated plasma into the temperature range of the particular EVE passbands that are sensitive to emission from lower temperature plasma.

Indeed, in the 2010 May 5 event for which Woods et al. (2011) conclude that secondary heating is likely, there is evidence that hot plasma was present during the initial energy release at the location of the source of the secondary emission up to an hour later (seen in AIA 94 Å emission, as presented by R. Hock et al. 2011, private communication). It is possible that the hot plasma cooled on timescales commensurate with conductive and radiative cooling times, as was the case in Aschwanden et al. (2009), who reported on post-flare EUV emission detected with *STEREO*/EUVI. They attribute the later EUV emission to the cooling of the soft-X-ray-emitting flare loops until they emit radiation detectable in the four spectral passbands covered by that instrument. In one well-observed event seen with both *STEREO-A* and *B*, they were able to estimate a ∼40 minute conductive and radiative cooling time of the stereoscopically imaged loops that they argued was consistent with the observed delay of 1 hr between the initial and secondary peaks in the soft X-ray and EUV light curves.

None of the events studied in Woods et al. (2011) had an increase in the *GOES* X-ray flux during the late phase. Can plasma be heated to a higher temperature than a few MK during the secondary heating phase (Woods et al. 2011) so that it can be detected in X-rays? In that case, a temperature diagnostic which can show the increase of plasma temperature in the second peak is critical evidence for a secondary heating phase.

In this letter, we present *SDO*/AIA, *STEREO*, *Reuven Ramaty High Energy Solar Spectroscopic Imager* (*RHESSI*), and *GOES* observations for a SEE that showed two *GOES* peaks separated by about 110 minutes and an associated two-stage CME eruption. This long time delay and increased plasma temperature (from 10 MK to 15 MK) at the time of the secondary peak demonstrate that the second peak could not be the result of the cooling of the plasma heated during the first peak, but was rather from a second episode of energy release. Additional evidence for this scenario comes from observations that show the EUV emission imaged with AIA, and the X-ray emission

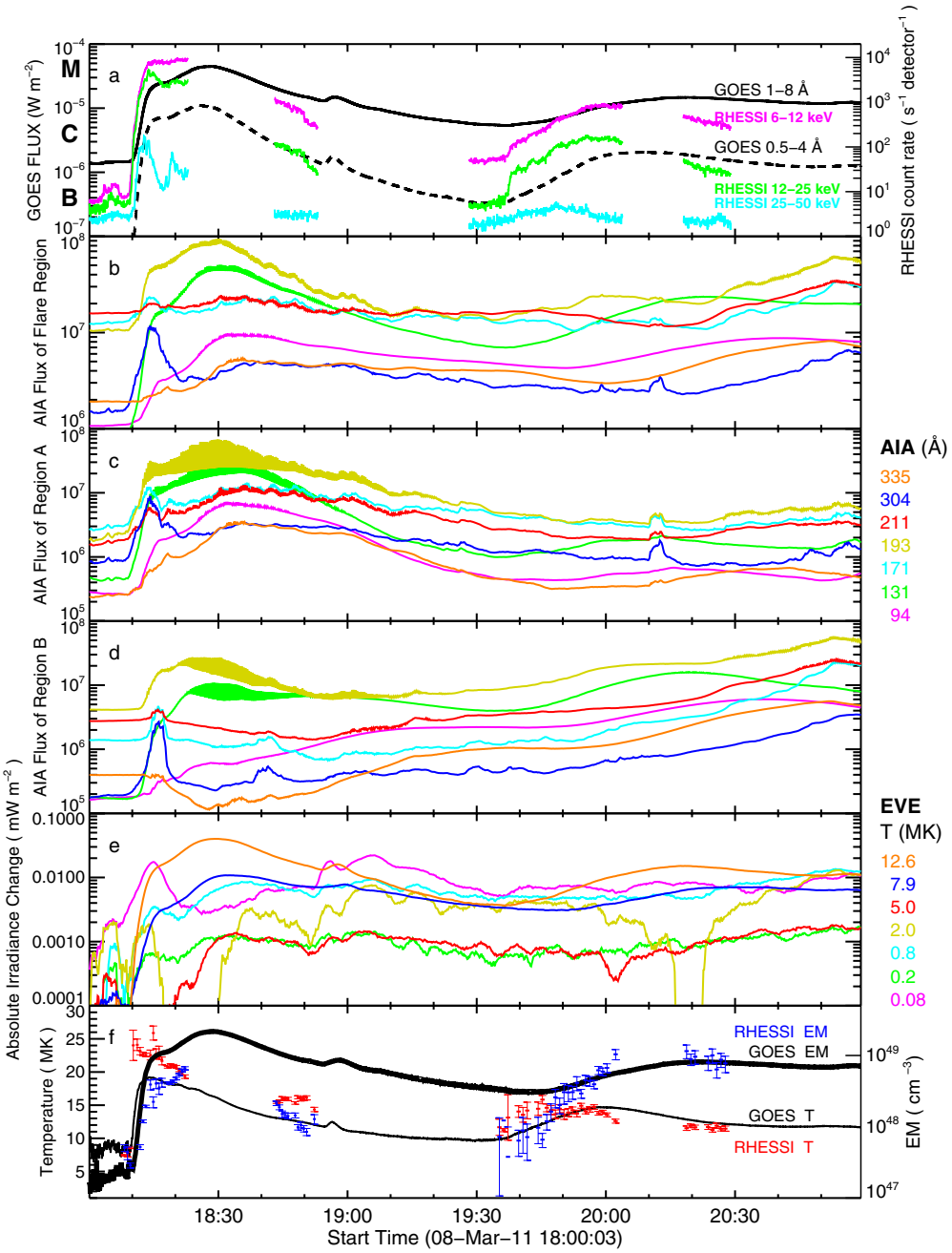

Figure 1. Light curves of the 2011 March 8 event: (a) *GOES* 1–8 Å (black solid line), 0.5–4 Å (black dashed line), *RHESSI* quick-look count rates from the front segments of detectors 1, 3, 4, 5, 7, and 8 at 6–12 keV (red), 12–25 keV (green, divided by 2 for clarity), and 25–50 keV (cyan, divided by 10). The peak at ∼18:56 UT was from a different active region close to disk center. (b) *SDO*/AIA flux in seven channels integrated over the entire flare region covering 400 × 500 arcsec^2. Each curve has a different constant flux subtracted for clarity. (c), (d) AIA flux integrated over Regions A and B shown in Figure 2, respectively. (e) The irradiance change at different temperatures derived from the *SDO*/EVE data. (f) Time evolution of plasma temperature (T) and emission measure (EM) derived from *GOES* and *RHESSI* data. The integration time for *RHESSI* spectra was 40 s before 19:30 UT and 60 s after.

(A color version of this figure is available in the online journal.)

imaged with *RHESSI* during the second stage, all come from about 40 arcsec above the site of the initial flare emission.

2. EVENT OVERVIEW

The event reported here occurred on 2011 March 8 on the southwest limb as seen from the Earth. It was well observed by a variety of instruments, including *RHESSI*, *SOHO*, *SDO*, *GOES*, *HINODE*, and Big Bear Solar Observatory. *STEREO-A* observed the event near disk center from a separation angle of 87° with Earth.

The AIA (Lemen et al. 2011) on the *SDO* images the solar atmosphere in 10 UV and EUV passbands covering temperatures from ∼5000 K to ∼20 MK with high spatial resolution (0.6 arcsec) and cadence (12 s). *RHESSI* (Lin et al. 2002) observes solar X-ray and gamma-ray emission above 3 keV with high cadence (4 s), spatial resolution (∼3 arcsec), and energy resolution (∼1 keV). It provides information on thermal plasma over ∼8 MK and accelerated electrons with energies above ∼10 keV. In addition, *STEREO-A* (EUVI; Wuelser et al. 2004) observed the EUV emission of the active region from above at 304, 171, 195, and 284 Å wavelengths with spatial

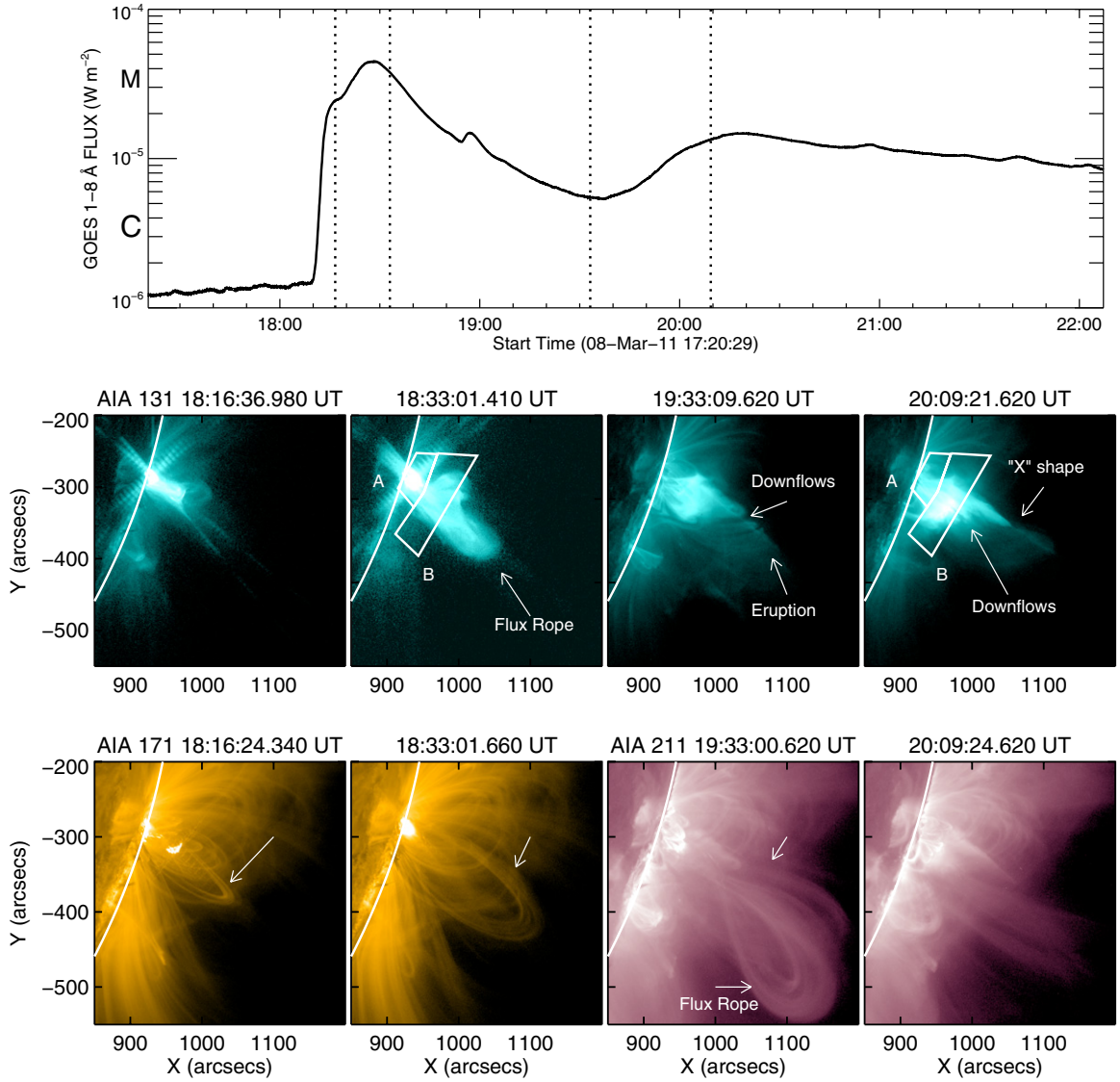

Figure 2. Top panel: *GOES* 1–8 Å light curve with dotted lines showing the times of the images below. Middle panel: AIA images in the 131 Å passband. The two white boxes marked as A and B show the two regions used to obtain the light curves in Figures 1(c) and (d). Bottom panel: images in the 171 and 211 Å passband with the three unlabeled arrows showing the location of expanding loops.

(An animation and a color version of this figure are available in the online journal.)

resolution of 1.6 arcsec and cadence from 75 s to 5 minutes. These four passbands observe mostly the plasma at temperatures from ∼0.1 to ∼2 MK, although the 195 Å channel has a secondary peak in sensitivity at log T(K) = 7.2.

Both the *RHESSI* and *GOES* X-ray light curves (see Figure 1(a)) show two peaks separated by almost 2 hr (∼108 minutes) that are identified as two individual M-class flares. The first peak (M4.4) started with an impulsive rise in the *GOES* 1–8 Å channel starting at 18:08 UT and peaking at 18:28 UT. The second, more gradual rise started at 19:46 UT, or even earlier if the decay of the X-ray flux from the first peak is subtracted, and peaked at the M1.4 level at 20:16 UT. The decay to background took about 4 hr. The small peak at ∼19:00 UT was from a different active region close to the disk center.

Seven AIA EUV light curves integrated over the entire flare region covering 400 × 500 arcsec^2 are shown in Figure 1(b). The AIA 131 Å passband (with a peak sensitivity at ∼0.5 MK and a secondary peak at ∼11 MK) best agrees with the *GOES* light curve (as pointed out by Cheng et al. 2011 and Woods et al. 2011). Figures 1(c) and (d) show the AIA flux integrated over Regions A and B in Figure 2, respectively. The light curves of AIA 94, 131, and 193 Å from Region B (higher altitude) all show an increase in their light curves during the first *GOES* peak, which indicates heating at the same time. The AIA 335 Å (∼3 MK) from Region B had a decrease during the first *GOES* peak and two gradual increases thereafter, which might be from the cooling of the plasma that produced the two *GOES* peaks, respectively. This idea is supported by the light curve of AIA 94 Å (∼6 MK) which also shows two gradual increases after the first *GOES* peak, but peaks earlier than the AIA 335 Å. This is different from the results of AIA 335 Å for the 2010 May 5 event in Woods et al. (2011), which shows only one peak after the *GOES* peak.

Figure 1(e) shows the irradiance change at different temperatures derived from the *SDO*/EVE data. The plasma temperatures (T) and emission measures derived independently from the two *GOES* channels and *RHESSI* spectra are shown in Figure 1(f). One isothermal component, one thick-target nonthermal

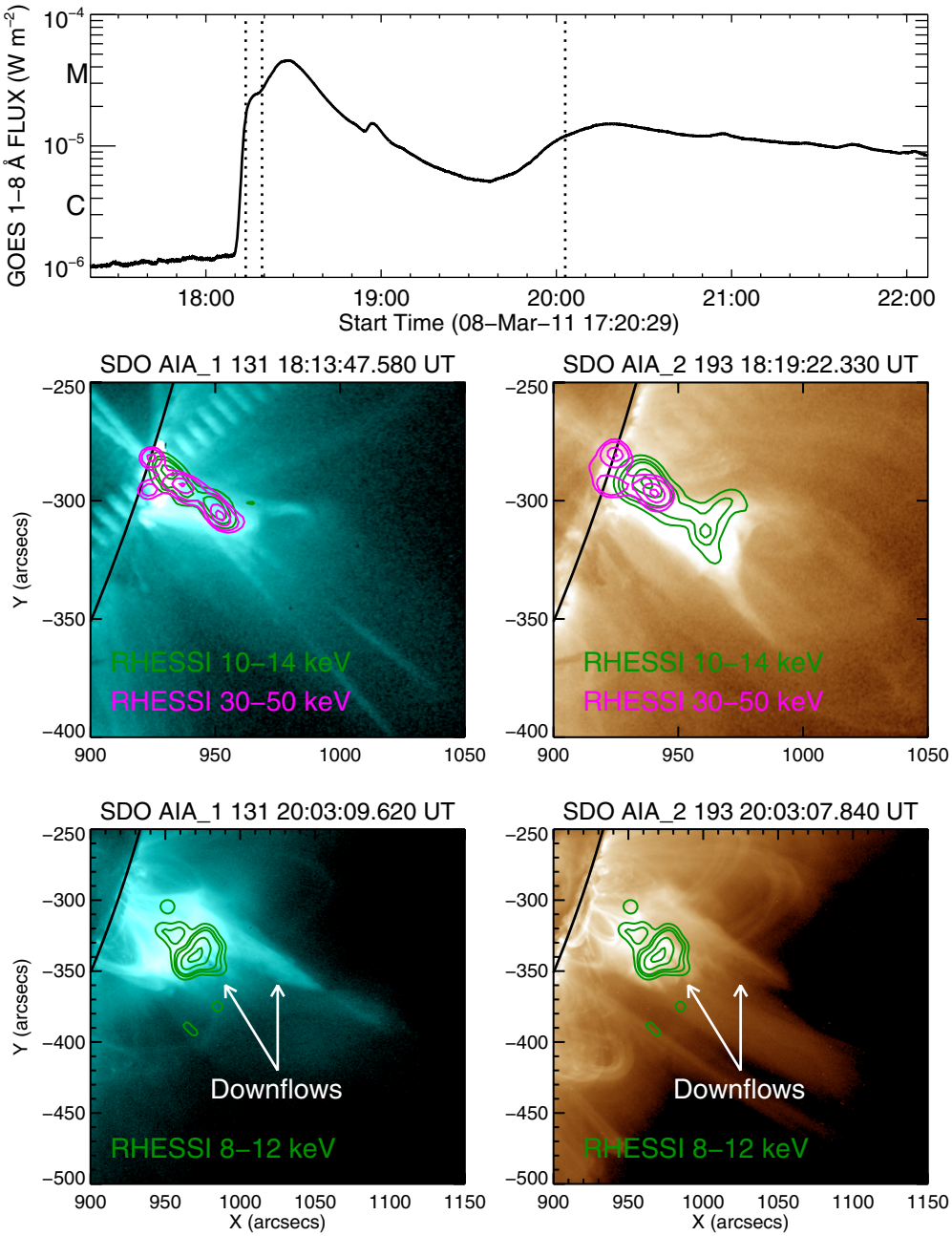

Figure 3. Top panel: same as Figure 2 but with different selected times. Middle and bottom panels: AIA 131 and 193 Å images and *RHESSI* thermal and nonthermal sources at three selected times. The *RHESSI* images were made using the Pixon and Clean algorithm with detectors 3, 4, 5, 8, and 9.

(An animation and a color version of this figure are available in the online journal.)

component (Thick2 in SSW/OSPEX), and two instrumental lines (when needed) were used to obtain acceptable spectral fits to the *RHESSI* data. Only the thermal component was needed for spectra in the decay phase around 18:45 UT. The *RHESSI* temperatures reached over 20 MK in the first peak and 15 MK in the second peak with similar values obtained from the *GOES* data. The increased irradiance at these high temperatures and at 12.6 and 7.9 MK as derived from EVE data shows that a heating phase must have occurred to produce the second *GOES* peak.

The two *GOES* peaks occurred in the same active region and appeared to be associated with the delayed eruption of a CME. Figure 2 shows *SDO*/AIA images from three channels, 131, 171 (∼0.6 MK) and 211 Å (∼2 MK), at four selected times, two during the first stage and two during the second stage (see the online animation for the entire event). These images show the formation of a hot flux rope during the first stage and the eruption of the same flux rope during the second stage.

2.1. First Stage, 18:10-19:30 UT, Formation of Flux Rope

The first stage was first observed in all AIA EUV channels when an eruption appeared above the limb at 18:10 UT. *RHESSI*'s 4–6 keV X-ray source was compact and low (about 10 arcsec above the limb) at this time and became extended toward the high corona following the erupting front (see Figure 3, middle panel, and the online animation). The bright structure (first image at 171 Å in Figure 2) reached a height of ∼55 arcsec above the limb at 18:16 UT. The loops ∼150 arcsec above the limb seen in 171 and 211 Å (first and second images in Figure 2 at 171 Å) started expanding and rising after the

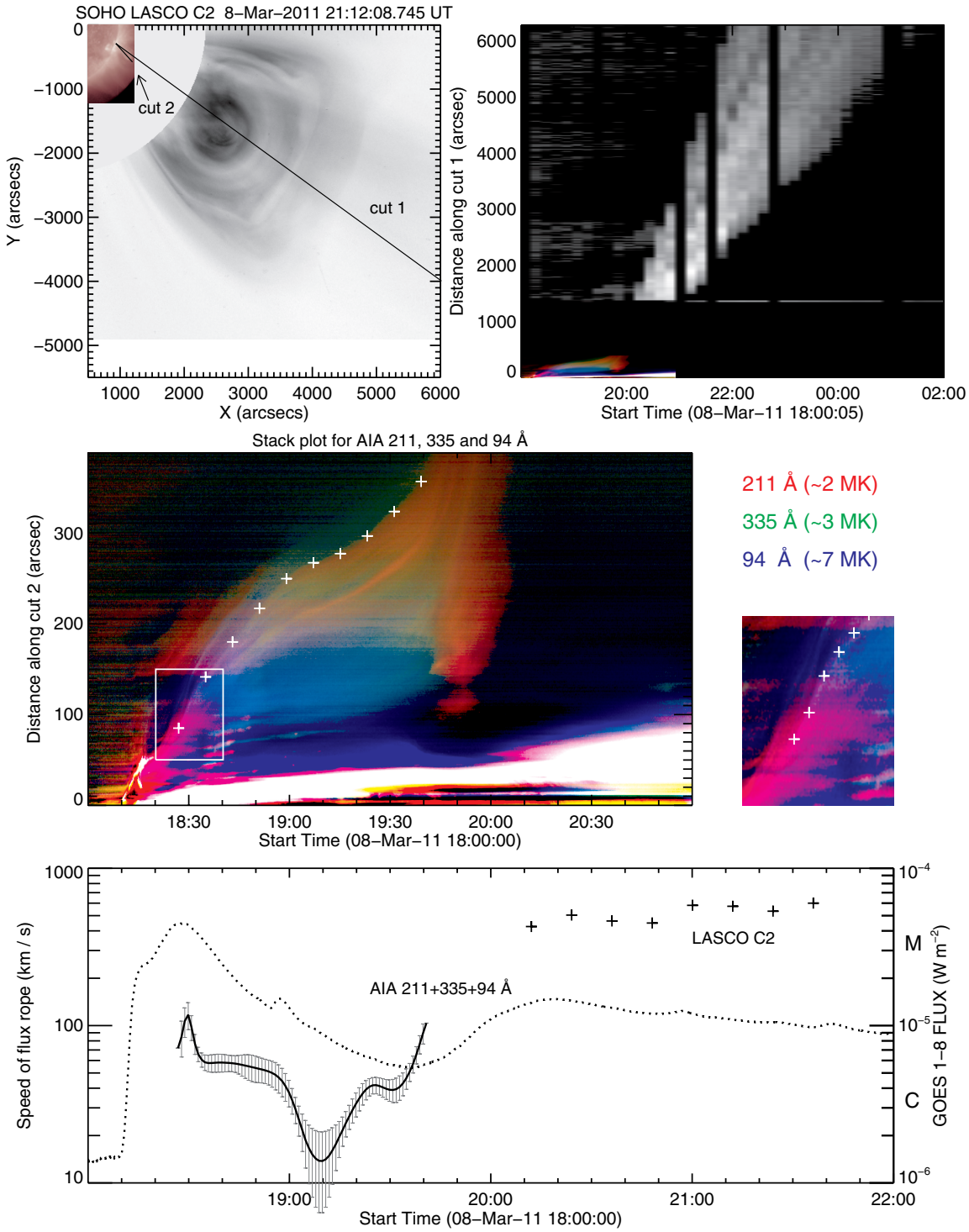

Figure 4. Flux rope and CME motion derived from *SDO*/AIA and *SOHO*/LASCO data. Top left panel: AIA 211 Å image and the CME observed by LASCO-C2 are shown on the left. The two "cuts" used for the stack plots are indicated by the two black lines. The stack plot in the top right panel shows the time evolution of flux along "cut 1." The black vertical lines are data gaps. Middle panel: stack plot of "cut 2" for AIA 211 (red), 335 (green), and 94 Å (blue). The image on the right shows the region marked in the left image. The crosses show the edge used to determine the speed of the flux rope. All the stack plots are from base difference images with the reference image at 18:00 UT. Bottom panel: speed of flux rope as a function of time with *GOES* 1–8 Å light curve. The $\pm 1\sigma$ errors on the speed are obtained from 10 independent measurements of the edge of the flux rope based on 1 minute cadence data.

(An animation and a color version of this figure are available in the online journal.)

eruption. *STEREO-A* also observed this expansion but these loops did not erupt as a CME.

The bright erupting feature seen in all AIA EUV channels separated into two parts at 18:15 UT. The upper part continued to rise but disappeared about 1 minute later and the lower part dropped back. A hot flux rope formed underneath the upper part continued to rise at a speed of ~70 km s^{-1}, accelerate to ~120 km s^{-1} at the *GOES* X-ray peak time, and then slowed down to about 14 km s^{-1} after 19:10 UT (see Figure 4). After 18:29 UT, the newly formed hot flux rope is visible in the

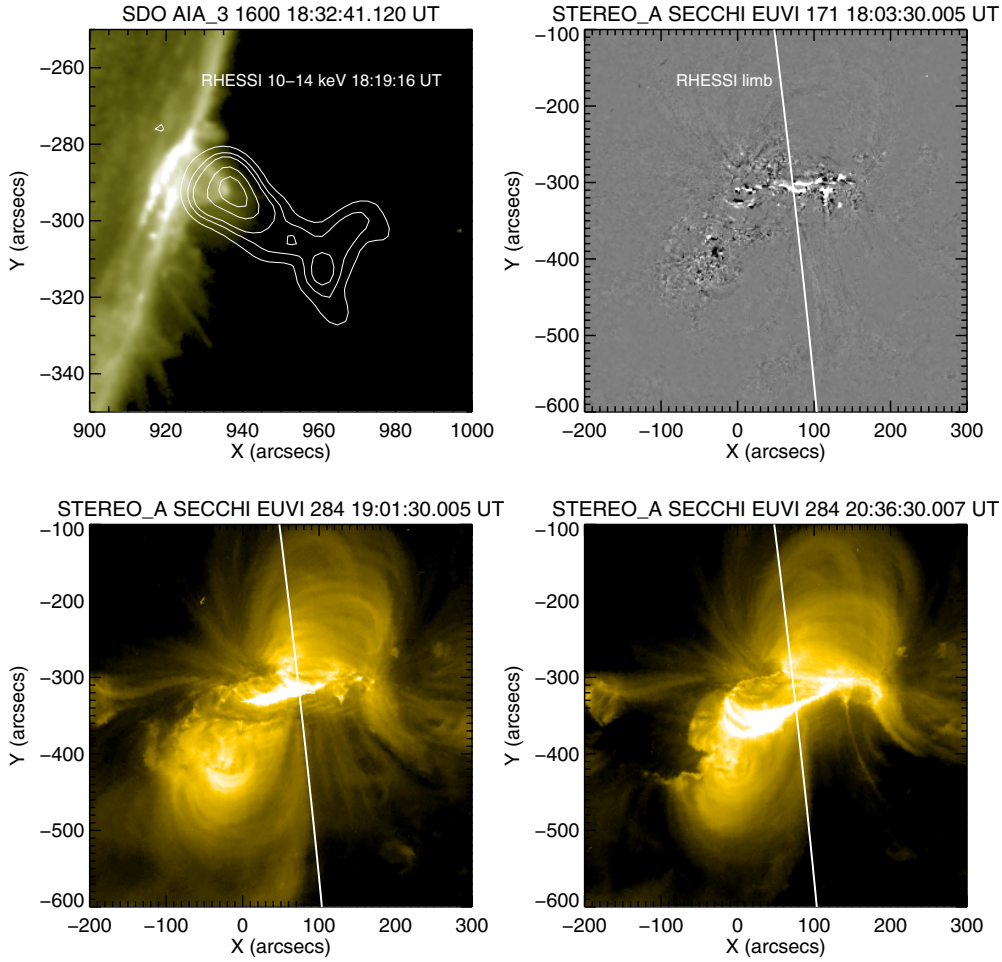

Figure 5. Top panel, left: AIA 1600 Å image (18:32 UT) showing parts of the two flare ribbons and flaring loops with *RHESSI*'s 10–14 keV contours (10, 20, 30, 60, and 90% of peak flux) at 18:19:16 UT. Top panel, right: *STEREO-A* 171 Å passband base difference image showing activity at 18:03:30 UT. The white lines in this image and the two below show the limb as seen from *SDO* and *RHESSI* in Earth orbit with the visible disk to the left. Bottom panel: *STEREO-A* 284 Å observations of post-flare loops during the two stages of the event.

(A color version of this figure is available in the online journal.)

AIA 131 Å (∼0.5 MK, 11 MK) image but not in AIA 171 Å (∼0.6 MK) (see the second image of AIA 131 and 171 Å in Figure 2). The sequence of appearance in different channels, from 131/94/193 to 335, then to 211, then to 193, and then to 171 Å, indicates that the flux rope cooled down from over 10 MK to ∼1 MK as it expanded and rose (see online animation and the color change from blue to green and then to red in the stack plot for AIA 211, 335, and 94 Å in Figure 4).

The hard X-rays (HXRs) above 25 keV had two major peaks during the first stage (Figure 1(a)), one at 18:13 UT and the other at 18:19 UT. At ∼18:14 UT, the 10–14 keV image shows a loop-top thermal source and an extended structure above it (the first image in Figure 3), while the high energy 30–50 keV image shows a similar elongated nonthermal source in the corona and emission from the flaring loops. At ∼18:19 UT, the time of the second HXR peak, the 10–14 keV source shows a Y-shaped structure high in the corona above the loop-top source, which agrees with the structure seen in AIA 193 Å images.

2.2. Second Stage, 19:30-00:40 UT, Eruption of the Flux Rope

The second stage started with an eruption around 19:33 UT seen in AIA 131 Å images after a build up of loops (third image at 131 Å in Figure 2). A fine bright line appeared at the start of the second peak (third image at 131 Å in Figure 2) followed by an elongated "X"-shaped structure (fourth image at 131 Å in Figure 2) initially with turbulence below, and later the appearance of rapidly falling new bright loops (see the online animation). Emission above the X-point was much fainter but suggested that hot plasma was also driven to higher altitudes at the same time.

The flux rope formed during the first stage accelerated again after ∼19:12 UT to about 100 km s^{-1} before it moved out of the AIA field of view. The average acceleration rate was about 0.11 km s^{-2} after 19:30 UT. It reappeared as the CME shown in the *SOHO*/LASCO image in Figure 4, first seen at 20:12 UT with an average speed of ∼516 km s^{-1}.

Downflows (McKenzie & Hudson 1999; Savage & McKenzie 2011) are clearly seen above the arcade region in AIA 193 Å images during the second stage (fourth image at 131 Å in Figure 2, and third and fourth images at 131 and 193 Å, respectively, in Figure 3). Plasma at lower altitude under the downflows and above the loops was heated at this time, resulting in an increase in the EUV emission from the higher temperature AIA passbands (131 and 193 Å, see Figures 1 and 3) and in the soft X-ray emission imaged by *RHESSI* (bottom panel in Figure 3). The *RHESSI* and *GOES* data show that the temperature peaked at ∼15 MK.

We do see a later peak in the AIA cooler channels (171, 211, 193, 304, and 335 Å) around 20:52 UT (Figure 1(b)). The fact that the flux in the 94 and 131 Å passbands peaked earlier than the fluxes in those cooler channels suggests that this peak in the cooler channels is from the cooling of the plasma heated in the second stage, although an additional heating episode in the same active region is not ruled out.

3. DISCUSSION

The eruptive event on 2011 March 8 had two stages, the first with impulsive X-ray emission and the second with more gradual emission. A hot flux rope (over 10 MK) formed in the first stage and rose with a speed of up to 120 km s^{-1} at ~18:30 UT. It cooled and slowed down to about 14 km s^{-1} but kept rising and expanding during the decay of the first *GOES* peak. The same flux rope accelerated again and erupted during the second stage, presumably to appear later as the CME seen with LASCO. At the same time, plasma was heated to about 15 MK at a location above the initial loop arcade formed during the first stage. *STEREO-A* observations (Figure 5) also show that the scale sizes of the flare loops in the second stage were larger than that of the loop arcade in the first stage. This is consistent with the findings of Woods et al. (2011) for the 2010 May 5 event. This two-stage eruptive event provides clear evidence for the secondary heating phase.

The differences between our results and those in Woods et al. (2011) are that not only the cooler EUV channels, but also the hotter EUV channels, *GOES*, and *RHESSI* responded to the second-stage energy release (Figure 1), and that the light curves of AIA 335 Å passband from the higher altitude (Region B) show two, rather than one, gradual peaks after the first *GOES* peak. We interpret these two gradual increases as results of the cooling of plasma that were heated to higher temperatures during the two stages. However, since the flux rope passed through the two regions (A and B), it may also contribute in the two light curves.

The base difference image in the *STEREO* 171 Å passband in Figure 5 shows a brightening at 18:03 UT, even before the start of the first peak. This observation suggests that the event started behind the limb and therefore gave a rapid rise in the *GOES* soft X-ray flux and temperature as the initial eruption emerged from behind the limb. In the first stage, *RHESSI* showed a 30–40 arcsec long X-ray source at both thermal and nonthermal energies extending up into the corona. AIA images in 131 and 193 Å show a similar structure. The *RHESSI* thermal sources show a Y-shaped coronal structure at 18:19 UT, similar to that seen in AIA 131 and 193 Å.

There are still many unanswered questions related to this event. Is the secondary heating always related to a delayed CME eruption? What is the reason for the decrease in velocity of the flux rope in the first stage? We will study this event in more detail and search for other similar events to answer these questions.

We thank the referee for providing valuable comments and help in improving this paper. We acknowledge the critical support provided by Kim Tolbert and Richard Schwartz and their help with the IDL *RHESSI* data analysis software and the SSW procedures. We are grateful to Frederick C. Bruhweiler for managing the NASA Grant NNG06GB96A at The Catholic University of America, through which one of us (Y.S.) was funded. This work is also supported in part by the European Community Framework Programme 7, "High Energy Solar Physics Data in Europe (HESPE)," grant agreement No. 263086. The work of T.W. was supported by NASA grants NNX08AE44G and NNX10AN10G.

REFERENCES

Aschwanden, M. J., Wuelser, J. P., Nitta, N. V., & Lemen, J. R. 2009, Sol. Phys., 256, 3
Cheng, X., Zhang, J., Liu, Y., & Ding, M. D. 2011, ApJ, 732, L25
Lemen, J. R., Title, A. M., Akin, D. J., et al. 2011, Sol. Phys., 275, 17
Lin, R. P., Dennis, B. R., Hurford, G. J., et al. 2002, Sol. Phys., 210, 3
McKenzie, D. E., & Hudson, H. S. 1999, ApJ, 519, L93
Savage, S. L., & McKenzie, D. E. 2011, ApJ, 730, 98
Shibata, K. 1998, in Observational Plasma Astrophysics: Five Years of YOHKOH and Beyond, ed. T. Watanabe & T. Kosugi (Astrophysics and Space Science Library, Vol. 229; Boston, MA: Kluwer), 187
Shibata, K., Masuda, S., Shimojo, M., et al. 1995, ApJ, 451, L83
Tsuneta, S. 1997, ApJ, 483, 507
Woods, T. N., Eparvier, F. G., Hock, R., et al. 2010, Sol. Phys., 275, 115
Woods, T. N., Hock, R., Eparvier, F., et al. 2011, ApJ, 739, 59
Wuelser, J.-P., Lemen, J. R., Tarbell, T. D., et al. 2004, Proc. SPIE, 5171, 111